Structure of Nanocomposite Hydrogel Investigated by Means of Contrast Variation Small-Angle Neutron Scattering

Hitoshi Endo,*,† Sho Miyazaki,†,§ Kazutoshi Haraguchi,‡ and Mitsuhiro Shibayama†

Neutron Science Laboratory, Institute for Solid State Physics, The University of Tokyo, 106-1 Shirakata, Tokai, Ibaraki 319-1106, Japan, and Kawamura Institute of Chemical Research, 631 Sakado, Sakura, Chiba 285-0078, Japan

Received February 21, 2008; Revised Manuscript Received May 14, 2008

ABSTRACT: The structure of poly(*N*-isopropylacrylamide)−clay nanocomposite gels (NC gel) is investigated. The sophisticated contrast variation small-angle neutron scattering technique leads to obtain the partial scattering functions of each component quantitatively. The extracted partial scattering functions of clay, polymer, and the polymer−clay cross-term are analyzed in detail, and the selective interaction between clay and polymer is revealed. On the basis of these structural observations, it is confirmed that the clay nanoparticles serve as 2-dimensional cross-linkers.

1. Introduction

"Nanocomposite" is a current key aspect for development of advanced materials,[1] e.g., polymer−clay nanocomposite in synthetic systems.[2] It is also well-known that the concept of *nanocomposite* is usually utilized in biological systems as organic−inorganic hybrid compounds,[3] e.g., bones, teeth, shells, etc. These materials are typically possessed of superior characters compared to conventional matters, for example, high mechanical property, low mass density, high refractive index, etc. These characters should occur by the mediation of the selective interaction between organic and inorganic components, and an understanding of the mechanism at the molecular level is very important in order to tune and optimize their properties.

Recently, polymer−clay nanocomposite hydrogels (NC gel) have been developed by Haraguchi et al.,[4−6] which have extraordinary superior properties to conventional hydrogels synthesized by using organic cross-linkers, such as large deformability with high elasticity, quick shrinkage after large deformation, nondestructivity, high optical transparency, and so on. Since the conventional hydrogels are very fragile, these characteristics of NC gels are great advantages for material use.

The NC gels are hybrid materials consisting of organic polymers and inorganic clay nanoparticles, which are synthesized by free-radical polymerization in the presence of clay nanoparticles without any organic cross-linkers. In order to elucidate the origin of the superior properties, various experimental approaches have been attempted. For example, Haraguchi et al. estimated the process of the NC gel formation by monitoring viscosity and optical transparency during the polymerization and also measured their mechanical properties by changing clay/polymer ratio and then suggested that the polymerization starts at the clay surfaces, and the polymer chains bridge between the different clay particles as the next step.[7] In this way, the clay nanoparticles may be functionalized as two-dimensional cross-linkers. Small-angle neutron scattering experiments (SANS) have been also performed for exploring their microscopic structures, and the sizes of polymer networks for the stationary and uniaxially stretched NC gels were estimated as a function of clay concentration.[8−10] These SANS experimental results support the role of clay nanoparticles as planar cross-linkers indirectly; however, the direct experimental evidence to confirm the idea is still lacking.

SANS with contrast variation or contrast matching is a very powerful tool for investigations of multicomponent nanocomposite systems, e.g., clay−polymer solutions,[11] silica−polymer suspension,[12] etc. In this paper, we want to invesitgate the detailed structure of NC gels by means of contrast variation small-angle neutron scattering. Our sophisticated contrast variation technique allows to decompose the observed intensities with different scattering contrasts into partial scattering functions of each component, i.e., clay, polymer, and solvent. Then detailed analyses of the obtained partial scattering functions lead to the elucidation of fine structural information on the system. Especially, the partial scattering functions contain the cross-terms, which directly reflect the pair correlation of the two components. We have applied the method to the NC gel in order to study sol−gel transition of the system, where the volume fraction of clay, ϕ_c, was very diluted ($\phi_c < 0.003$).[13] Since more concentrated clay was contained in the system for this study ($\phi_c = 0.013$), the synthesized NC gel was quite elastic.[5] Differently from our previous study in ref 13, a structure factor must be taken into account in order to analyze the partial scatterig functions quantitatively. The evaluated structure factor directly gives information on the interaction in the system, e.g., the interaction between clay particles; therefore, quantitative investigation of the structure factor is very important. We will determine below the detailed structure of NC gel with $\phi_c = 0.013$ and reveal the selective interaction between clay and polymer by theoretical evaluation of the self-correlations of clay and polymer as well as the cross-correlation between clay and polymer.

2. Scattering Theory

2.1. Partial Scattering Functions and Contrast Variation. In the case of the NC gels, the scattering intensities can be described with partial scattering functions $S_{ij}(Q)$ by

$$I(Q) = \Delta\rho_c{}^2 S_{cc}(Q) + 2\Delta\rho_p \Delta\rho_c S_{cp}(Q) + \Delta\rho_p{}^2 S_{pp}(Q) \qquad (1)$$

where $S_{cc}(Q)$ and $S_{pp}(Q)$ are the self-terms of clay and polymer, respectively, and $S_{cp}(Q)$ is the cross-term between clay and polymer. Here, $\Delta\rho_i$ (with $i = c$ and p for clay and polymer, respectively) is the scattering contrast between the component i and water as the solvent, and Q is the magnitude of the

* To whom correspondence should be addressed. E-mail: hit-endo@issp.u-tokyo.ac.jp.
† The University of Tokyo.
‡ Kawamura Institute of Chemical Research.
§ Current address: New Products Development Center, Technology Development Div. AGC Automotive Japan/Asia Pacific, Asahi Glass Co., LTD. 1 Aza Asahi, Taketoyo-cho, Chita-gun Aichi 470-2521, Japan.

10.1021/ma800390p CCC: $40.75
Published on Web 06/18/2008

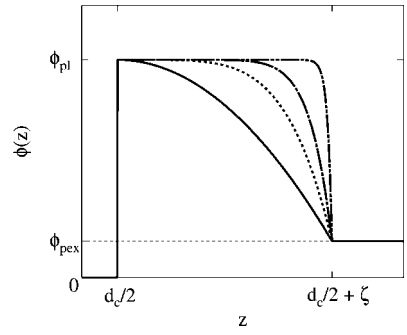

Figure 1. Polymer density profiles perpendicular to the clay surface for different h in eq 11. $z = d_c/2$ corresponds to the interface between clay and adsorbed layer. The curves correspond to $h = 2$ (solid), 5 (dotted), 10 (dashed-dotted), and 50 (dashed-two dotted).

scattering vector, i.e., $Q = 4\pi \sin(\Theta/2)/\lambda$ with the scattering angle Θ and the neutron wavelength λ. The dimensions of the scattering contrast are inverse of length squared, so that the partial scattering function possesses a dimension of volume in this definition. Since $S_{cp}(Q)$ directly reflects the interaction between the clay particles and the polymer chains in the hybrid gel, we can determine the cross-correlation between these two components by evaluating $S_{cp}(Q)$. In order to extract these three partial scattering functions, three different scattering length densities of water, ρ_w, are the minimum requirement. Therefore, the seven different water contrasts, corresponding to the compositions shown in Figure 2, occur over determination, which can improve the reliability of the decomposition of the measured intensities into each partial scattering function and be solved by singular value decomposition separately for each Q value. The detailed theoretical as well as experimental description of the contrast variation SANS can be found elsewhere.[14]

2.2. Scattering Function for Clay, $S_{cc}(Q)$. Since the form of the Laponite nanoparticle is known as disk-shaped,[4,5] the form factor of clay, $P_c(Q)$, with a bottom radius R_c and thickness d_c is given by

$$P_c(Q) = \int_0^{\pi/2} \{A_c(Q)\}^2 \sin\theta \, d\theta \tag{2}$$

where $A_c(Q)$ is the scattering amplitude of clay, i.e.

$$A_c(Q) = V_c \frac{2J_1(QR_c \sin\theta)}{QR_c \sin\theta} \frac{\sin(Qd_c \cos\theta/2)}{Qd_c \cos\theta/2} \tag{3}$$

with the cylindrical Bessel function of first order J_1. V_c is the volume of a clay platelet

$$V_c = \pi {R_c}^2 d_c \tag{4}$$

and $\int_0^{\pi/2} \sin\theta \, d\theta$ in eq 2 represents random orientation of the clay platelets. Here, θ is the angle between a reference axis and the principal axis of the disk.

It is known that the structure factor, $S(Q)$, is affected by the orientation of the anisotropic scattering amplitudes.[15] In this case, $S(Q)$ should be modified as

$$S(Q) \rightarrow S_c(Q) = 1 + \frac{\langle A_c(Q)\rangle^2}{P_c(Q)}\{S(Q) - 1\} \tag{5}$$

in which

$$\langle A_c(Q)\rangle = \int_0^{\pi/2} A_c(Q) \sin\theta \, d\theta \tag{6}$$

The $S(Q)$ should be appropriately chosen, which will be discussed below.

Therefore, the partial scattering function of clay, $S_{cc}(Q)$, is defined by

$$S_{cc}(Q) = n_c S_c(Q) P_c(Q) \tag{7}$$

with the number density of clay particles n_c.

2.3. Scattering Function for Polymer, $S_{pp}(Q)$. In order to calculate the partial scattering function of polymer, $S_{pp}(Q)$, we assume that the polymer chains are adsorbed onto the surface of clay nanoparticles. The effect of the nonadsorbed external polymer chains will be discussed later in section 4. In this case, the form factor of the polymer adsorption layer, $P_p(Q)$, can be calculated as follows:

$$P_p(Q) = \int_0^{\pi/2} \{A_{p\parallel}(Q \sin\theta)\}^2 \{A_{p\perp}(Q \cos\theta)\}^2 \sin\theta \, d\theta \tag{8}$$

with the scattering amplitudes of the polymer adsorption layer for the parallel direction of the clay surface, $A_{p\parallel}(Q)$, and the perpendicular direction, $A_{p\perp}(Q)$, which are described as

$$A_{p\parallel}(Q) = \frac{2J_1(QR_p)}{QR_p} \tag{9}$$

where R_p is the radius of the polymer layer and

$$A_{p\perp}(Q) = \int_0^{\infty} \phi(z) \cos(Qz) \, dz \tag{10}$$

In eq 10, $\phi(z)$ represents the density profile of polymer segments perpendicular to the clay surface. In this study, the density profile

$$\phi(z) \propto 1 - (z/\zeta)^h \quad (0 \le z \le \zeta, 1 < h) \tag{11}$$

with the layer thickness, ζ, and exponent, h, is applied. The model with $h = 2$ was suggested by Millner et al. for end-grafted polymer brush,[16] and $h \rightarrow \infty$ leads to the step function with the layer thickness ζ. Figure 1 depicts the profiles of $\phi(z)$ for different h. Then the scattering amplitude $A_{p\perp}(Q)$ can be obtained by Fourier transformation of $\phi(z)$ along the z-axis. The normalized $A_{p\perp}(Q)$ is derived as

$$\begin{aligned} A_{p\perp}(Q) &= \left\{\frac{d_c}{2} + \frac{h\zeta}{1+h}\right\}^{-1}\left[\int_0^{d_c/2} \cos(Qz) \, dz + \right. \\ &\quad \left. \int_{d_c/2}^{d_c/2+\zeta} \left\{1 - \left(\frac{z - d_c/2}{\zeta}\right)^h\right\} \cos(Qz) \, dz\right] \\ &= \zeta\left\{\frac{d_c}{2} + \frac{h\zeta}{1+h}\right\}^{-1}\left[\int_0^1 k^h \sin(Q\zeta k) \, dk \sin\left(\frac{Qd_c}{2}\right) - \right. \\ &\quad \left. \int_0^1 k^h \cos(Q\zeta k) \, dk \cos\left(\frac{d_c Q}{2}\right) + \sin\left\{Q\left(\frac{d_c}{2} + \zeta\right)\right\}\Big/(Q\zeta)\right] \end{aligned} \tag{12}$$

In the case of $h = 2$, eq 12 can be simplified as

$$\begin{aligned} A_{p\perp}(Q) = \frac{12}{Q^3\zeta^2(3d_c + 4\zeta)}\left[\sin\left\{Q\left(\frac{d_c}{2} + \zeta\right)\right\} - \right. \\ \left. \sin\left(\frac{Qd_c}{2}\right) - Q\zeta \cos\left\{Q\left(\frac{d_c}{2} + \zeta\right)\right\}\right] \end{aligned} \tag{13}$$

and $h \rightarrow \infty$ leads to

$$A_{p\perp}(Q) = \frac{\sin\{Q(d_c/2 + \zeta)\}}{Q(d_c/2 + \zeta)} \tag{14}$$

Equations 9 and 12 contain the amplitude from the clay platelet, which must be subtracted. Therefore, the scattering amplitude of the polymer layer $A_p(Q)$ is given by

$$A_p(Q) = (\phi_{pl} - \phi_{pex}) V_p A_{p\parallel}(Q \sin\theta) A_{p\perp}(Q \cos\theta) - \phi_{pl} V_c A_c(Q) \tag{15}$$

with the volume fraction of the polymer segments in the layer swollen with solvents, ϕ_{pl}, and the volume fraction of polymer segments out of the layer, ϕ_{pex} (see Figure 1). V_p is the volume of the layer, i.e.

$$V_p = \pi R_p^2 \left(d_c + \frac{2h\zeta}{1+h} \right) \tag{16}$$

Finally, eq 8 is redefined as

$$P_p(Q) = \int_0^{\pi/2} \{A_p(Q)\}^2 \sin\theta \, d\theta \tag{17}$$

with eq 15.

The partial scattering function of polymer, $S_{pp}(Q)$, is then described as

$$S_{pp}(Q) = n_c P_p(Q) \left[1 + \frac{\langle A_p(Q) \rangle^2}{P_p(Q)} \{S(Q) - 1\} \right] \tag{18}$$

in the same way as in eq 5, where $\langle A_p(Q) \rangle$ is defined as

$$\langle A_p(Q) \rangle = \int_0^{\pi/2} A_p(Q) \sin\theta \, d\theta \tag{19}$$

2.4. Scattering Function for Clay−Polymer Cross-Term, $S_{cp}(Q)$. The cross-term between clay and polymer, $S_{cp}(Q)$, reflects the cross-correlation between clay and polymer. We are discussing the case in which the polymer chains attach to the clay surfaces. In this case, $S_{cp}(Q)$ may be described as

$$S_{cp}(Q) = n_c [\langle A_c(Q) A_p(Q) \rangle + \langle A_c(Q) \rangle \langle A_p(Q) \rangle \{S(Q) - 1\}] \tag{20}$$

where

$$\langle A_c(Q) A_p(Q) \rangle = \int_0^{\pi/2} A_c(Q) A_p(Q) \sin\theta \, d\theta \tag{21}$$

with eqs 3, 6, 15, and 19.

2.5. Structure Factor. For appropriate description of the structure factor, the Percus−Yevick (PY) theory[17−19] may be applied. Rigorously, the PY theory is for the hard-core systems with spheres; therefore, the application of the PY theory to the NC gels should be carefully discussed. However, it is known that the Laponite clay nanoparticles are weakly charged;[7] the adsorbed polymer chains on the clay particles can strongly screen the charge, so that the electrostatic interaction may be negligible in the system. Our system is very diluted (volume fraction of 1.3% for clay), and the average distance between the nearest-neighbor centers of mass of the clay particles is about 400 Å, which is estimated by the assumption that each particle occupies cubic space, so that the orientation of the particles would not be affected by any strong steric interparticle interactions. Moreover, the clay particles would be confined by the polymer networks. Therefore, the anisotropic shape of clay nanoparticles may be also neglected, and the PY theory may approximate the repulsive interaction. The PY theory is represented by the radius of a hard-core sphere R_{PY} and its total volume fraction ϕ_{PY}, i.e.

$$\phi_{PY} = n_c \frac{4\pi R_{PY}^3}{3} \tag{22}$$

with the number density of clay particles, n_c. In our case, $d_c < 2R_{PY} < 2R_c$ would be expected, so that R_{PY} should be estimated independently of R_c and d_c. The other useful descriptions about the PY theory are given elsewhere.[20,21]

3. Experiment

In this study, the NC gels were prepared by free-radical polymerization of *N*-isopropylacrylamide (NIPAM) monomer in aqueous solution under the coexistence of synthetic clay nanoparticles, Laponite XLG (Rockwood Ltd.: $[Mg_{5.34}Li_{0.66}Si_8O_{20}(OH)_4]$-$Na_{0.66}$). The prereaction solution consisted of 0.045 M clay as well as 0.47 M NIPAM monomer in the aqueous solution, where oxygen was removed by bubbling N_2 gas. Therefore, the synthesized NC gels consisted of 4.2 vol % polymer and 1.3 vol % clay; i.e., the volume fraction of water was more than 90%, which were prepared in planar quartz cells for scattering experiments, and the dimension was 1 or 2 mm thickness (depending on the sample transmission) × 10 mm width × 30 mm height. Potassium persulfate and *N,N,N′,N′*-tetramethylethylendiamine were used as initiator and catalyst, and the polymerization started by increasing the temperature from ice−water to room temperature (around 20 °C) and proceeded for more than 24 h. The other deteiled description of the synthesis is given elsewhere.[4,5]

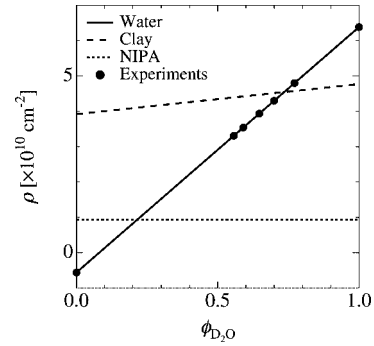

Figure 2. Scattering length densities of water (solid), clay (broken), and polymer (dotted) as a function of D_2O volume fraction in aqueous solution, ϕ_{D_2O}. The experimental conditions are marked by filled circles on the solid line.

Small-angle neutron scattering (SANS) experiments were performed on NC gels at 20 °C by SANS-U diffractometer of Institute for Solid State Physics, the University of Tokyo, locating at JRR-3 M research reactor of Japan Atomic Energy Agency in Tokai, Japan.[22] The experiments were carried out at sample-to-detector distances of $L = 2$ and 8 m using a neutron wavelength 7 Å with $\Delta\lambda/\lambda$ = ca. 10% full width at half-maximum. The corresponding Q range was from 0.0045 to 0.15 Å^{-1}.

Each data set was normalized to absolute intensity by the incoherent scattering of a polyethylene thin plate as a standard sample after the necessary data corrections such as air scattering, cell scattering, and incoherent scattering subtraction.

Contrast variation techniques can be easily executed with neutrons as probe, which is based on hydrogen/deuterium replacement in order to modify the scattering visibility of different components in the system. Since the scattering length densities of NIPAM ($\rho_p = 0.933$ [× 10^{10} cm^{-2}], the corresponding mass density is 1.26 g/cm^3) and clay ($\rho_c = 3.92 + 0.85 \times \phi_{D_2O}$ [× 10^{10} cm^{-2}], the corresponding mass density is 2.65 g/cm^3; ϕ_{D_2O} is the volume fraction of D_2O in water) are well separated, the contrast variation experiments may be realized by only changing the scattering length density of solvent (water), ρ_w, i.e., $\rho_w = 6.95 \times \phi_{D_2O} - 0.56$ [× 10^{10} cm^{-2}], where the correponding mass density of protonated water is 1.00 g/cm^3. The dependence of ϕ_{D_2O} on the scattering length density of the clay is due to hydrogen/deuterium exchange at hydroxyl groups. In this experiments, $\phi_{D_2O} = 0$, 0.557, 0.591, 0.647, 0.700, 0.772, and 1.00 were applied, where the corresponding scattering length densities of water are $\rho_w = -0.559$, 3.31, 3.54, 3.94, 4.30, 4.80, and 6.39 [× 10^{10} cm^{-2}], respectively. The volume fractions for each component in these seven samples were prepared to be identical as precise as possible, which was the minimal requirement to perform the contrast variation experiment. Since the strong affinity between the monomers and the clay surfaces is dominant for NC gel formation, the H_2O/D_2O mixing effect for the sample preparation may be negligible. It is also known that the volume phase transition of NIPAM polymer is affected by the H_2O/D_2O mixing,[23] but our system is far away from the transition temperature, so that this effect is negligible, too. Figure 2 shows the scattering length densities of the components as a function of ϕ_{D_2O}, where the measured conditions are marked by filled circles. It is clearly shown that the contrast variation experiment was designed in order to cover the matching contrast between clay and water ($\phi_{D_2O} = 0.73$). As incoherent scattering disturbed the coherent signal considerably at the matching contrast between polymer and

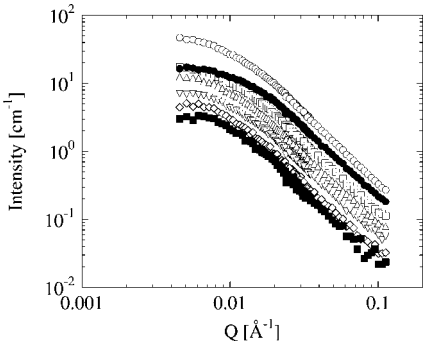

Figure 3. Scattering intensities of the NC gel obtained for the different contrast by tuning D_2O/H_2O ratio. The curves correspond to ϕ_{D_2O} = 1.00 (○), 0.772 (□), 0.700 (Δ), 0.647 (▽), 0.591 (◇) 0.557 (■), and 0 (●), where ϕ_{D_2O} is the volume fraction of D_2O in the aqueous solution.

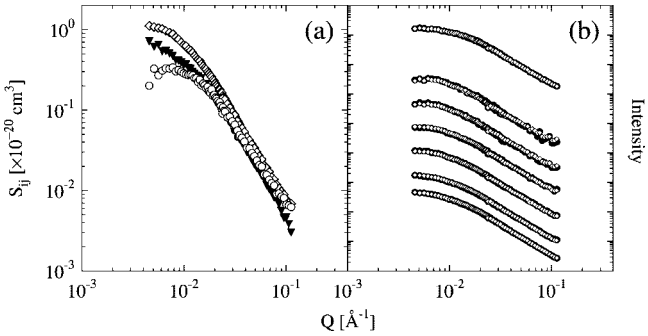

Figure 4. (a) Obtained partial scattering functions of clay, S_{cc} (○), clay−polymer cross-term, S_{cp} (▼), and polymer, S_{pp} (◇). (b) Reconstructed scattering curves (◇) compared to the experimental values (●). The curves are shifted each other by an additional scaling factor of 10 for better visualization. The lowermost curves are obtained from the sample with ϕ_{D_2O} = 1.00, and the corresponding ϕ_{D_2O} decreases from bottom to top.

water (ϕ_{D_2O} = 0.21), the measurements around the clay−water matching point were more efficient for obtaining the partial scattering functions with high reliability.

4. Results and Discussion

Figure 3 shows the scattering intensities observed in the contrast variation experiments for the seven samples, whose structures were identical, and the scattering length density of aqueous solution was varied by tuning the volume fraction of D_2O in the solvents, ϕ_{D_2O}. The highest average scattering intensity was obtained from the sample with 100% D_2O solvent, and the sample with pure H_2O solvent was the second. The others decreased as the scattering length density of water decreased; i.e., ϕ_{D_2O} decreased. Therefore, the minimum of the average intensities located not near the matching point between water and clay (ϕ_{D_2O} = 0.73) but the matching point between water and polymer (ϕ_{D_2O} = 0.21). This result suggests that the partial scattering function of polymer must be more intense than that of clay, which would be due to aggregation of the polymer chains in the NC gel.

The achieved partial scattering function of clay, $S_{cc}(Q)$, polymer, $S_{pp}(Q)$, and clay−polymer cross term, $S_{cp}(Q)$, as well as the reconstructed scattering curves are exhibited in Figure 4. The reconstruction of scattering curves was done from the obtained partial scattering functions and the estimated scattering length densities. It is clearly seen that the relation of $S_{pp}(Q) > S_{cc}(Q)$ is held in Figure 4a as mentioned above. The cross-term $S_{cp}(Q)$ is positive, and the magnitude is between $S_{cc}(Q)$ and $S_{pp}(Q)$. The positive $S_{cp}(Q)$ indicates that the clay surfaces attract

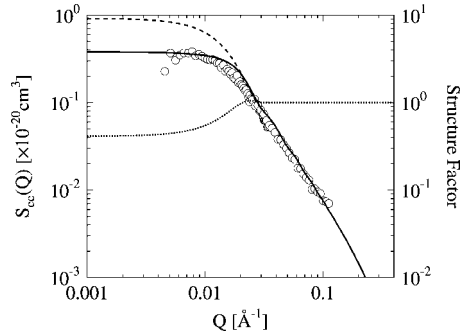

Figure 5. Partial scattering function of clay, $S_{cc}(Q)$ (○). The solid curve indicates the fitting result. The broken curve and the dotted curve show the intensity with only form factor, $P_c(Q)$, (i.e., $S_c(Q)$ = 1 in eq 7) and the structure factor, $S_c(Q)$, given in eq 5, respectively, which are extracted from the fitting curve (the solid curve). The right axis indicates the magnitude of the structure factor.

the polymer chains and the clay platelets are surrounded by dense polymer chains. This point will be discussed in detail below. Figure 4b depicts the good agreements between the reconstructed and experimental data, which confirms the good reliablility of the SANS experiments as well as the estimation of the scattering contrasts.

In order to reveal the structure of the NC gels quantitatively, the partial scattering functions were analyzed individually step by step.

At first, $S_{cc}(Q)$ was evaluated quantitatively. Since the shape of laponite was known as a nanoplatelets of the order of thickness d_c = 10 Å and radius R_c = 150 Å,[8] the number density, n_c, could be calculated from the volume fraction. Therefore, the form factor of the clay nanoparticles, $P_c(Q)$, could be computed by eq 7 with $S_c(Q)$ = 1. In Figure 5 the observed $S_{cc}(Q)$ and the result of numerical computation are compared, where the dotted curve indicates the computed $P_c(Q)$. At high Q the calculated value coincided with $S_{cc}(Q)$ very well, which confirmed that the estimations of n_c and $P_c(Q)$ were very precise. As the overshoot of the calculated $P_c(Q)$ at low Q indicated repulsive interaction of the clay nanoparticles, the particle should exist individually in the system, and any possibilities of their major aggregations were ruled out in the system with clay volume fraction ϕ_c = 0.013. Therefore, the effect of the repulsive interaction should be considered, which represents by the structure factor, and the Percus−Yevick theory was chosen in order to calculate the structure factor as discussed in section 2.5. The solid curve in Figure 5 shows the fiiting result with eq 7 which could reproduce the experimental data very well. The free parameter was only R_{PY} within eq 22, and R_{PY} = 113 Å was evaluated.

The cross-term between clay and polymer, $S_{cp}(Q)$, was evaluated as the second step. We emphasize again that the cross-term can be experimentally obtained by only using this contrast variation method, and $S_{cp}(Q)$ directly gives us the correlation between clay and polymer in the NC gels. Especially the sign and amplitude of the cross-term reflect the magnitude of their interaction.[24] If the polymer chains are repulsive from the clay nanopartiles, i.e., $\phi_{pl} < \phi_{pex}$ in eq 20, it is clear that $S_{cp}(Q)$ becomes negative. If there is no correlation between the clay and the polymer, the intensity of $S_{cp}(Q)$ is null or experimentally imperceptible. In the case that the polymer chains are attached to the clay particles and they are repulsive from the surfaces, $S_{cp}(Q)$ must oscillate from positive at low Q to negative at high Q with attenuating.[25,26] Therefore, the observed positive $S_{cp}(Q)$ with intense magnitudes can be concluded that the interaction between the polymer chains and the clay particles is very attractive, and each clay nanoparticle is covered with the dense polymer layer.

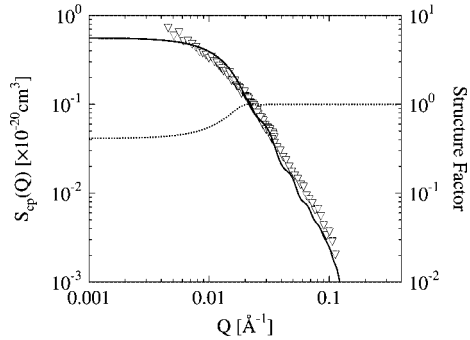

Figure 6. Partial scattering function of clay−polymer cross-term, $S_{cp}(Q)$ (▽). The solid curve indicates the fitting result with eq 20, and the corresponding structure factor is shown by the dotted curve, whose magnitude is indicated by the right axis.

The obtained cross-term between clay and polymer, $S_{cp}(Q)$, is exhibited in Figure 6. The solid curve is the result of the fitting with eq 20, and the corresponding structure factor is depicted by the dotted curve in Figure 6, which could be evaluated by $1 + \langle A_c(Q)\rangle\langle A_p(Q)\rangle/\langle A_c(Q)A_p(Q)\rangle\{S(Q) - 1\}$ in eq 20. In this case, the position of the center of mass for the clay particle coincides with that of the adsorbed polymer layer, so that R_{PY} evaluated by $S_{cc}(Q)$ should be the same as those for $S_{cp}(Q)$ as well as $S_{pp}(Q)$. Therefore, the all parameters determined by the fitting of $S_{cc}(Q)$, i.e., d_c, R_c, n_c, and R_{PY}, were used as they were for the evaluations of $S_{cp}(Q)$, and the free parameters were the radius of the adsorbed polymer layer, R_p, the layer thickness, ζ, the exponent for the polymer density profile, h (see eq 11), and the polymer volume fraction in the adsorbed layer, ϕ_{pl}, in eq 15. The fitting curve could reproduce the experimental results fairly well as same as the case of $S_{cc}(Q)$, and the evaluated values were $R_p = 219$ Å, $\zeta = 10$ Å, $h = 5.3$, and $\phi_{pl} = 0.35$. The volume fractions ϕ_{pl} and ϕ_{pex} are related to the total polymer volumer fraction, Φ_p, as

$$\phi_{pex} = \frac{\Phi_p - n_c\phi_{pl}(V_p - V_c)}{1 - n_cV_c} \tag{23}$$

where n_c is the number density of the clay particles and V_{clp} is defined by eq 4 or eq 16. From the fitting $\phi_{pl} = 0.35$ and $\phi_{pex} = 0.022$ were evaluated; therefore, the adsorbed layer is more than 10 times denser compared to the external polymer concentration. In the case of end-grafted polymers, $h = 2$ in eq 11 is suggested,[16] while the obtained $h = 5.3$ in this study suggests a step-function-like profile (see Figure 1). This may be due to strong attractive interaction between the clay and the polymer. These results directly confirm that the polymers are strongly anchored to the clay surfaces; thus, the clay nanoplatelets work as planar cross-linkers.

We expect that the attractive interaction is realized by hydrogen bond; therefore, the NC gel may be a kind of physical gel. However, the origin of the formation of attractive interaction has not been clearly understood yet. Since the NC gels do not form by simple mixing of NIPAM polymers and the clay particles, the synthetic process may be very important.[7]

The obtained radius of the adsorbed layer, R_p, was roughly 70 Å larger than that of the clay, which may arise from the assumption of the shape of the adsorbed layer and the structure factor. By applying more complex models, more reasonable R_p might be obtained.

Finally, $S_{pp}(Q)$ was evaluated with eq 18 on the basis of the analyses of $S_{cc}(Q)$ and $S_{cp}(Q)$. Since the all necessary parameters for the calculation of eq 18 were already achieved from the analyses of $S_{cc}(Q)$ and $S_{cp}(Q)$, we could directly calculate the corresponding scattering intensity for the polymer−polymer

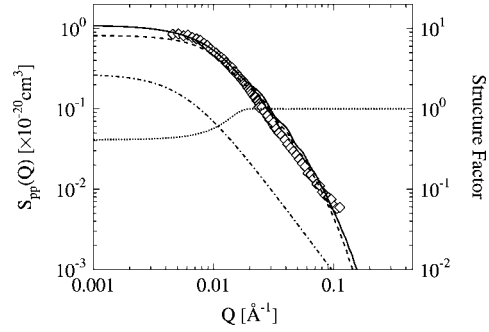

Figure 7. Partial scattering function of polymer, $S_{pp}(Q)$ (◇). The broken curve indicates the fitting result with eq 18. The dashed-dotted curve exhibits the contribution of a Lorentz function in eq 24, and the total fitting curve given by eq 24 is shown by the solid curve. The corresponding structure factor evaluated by the equation in the square brackets in eq 18 is shown by the dotted curve, where the magnitude is given by the right axis.

Table 1. Evaluated Fitting Parameters in This Study[a]

	ϕ_c	R_c	d_c	R_{PY}
$S_{cc}(Q)$	0.013	150 Å	10 Å	113 ± 1 Å
	R_p	ζ	Φ_p	h
$S_{cp}(Q)$	219 ± 1Å	10 ± 1Å	0.35 ± 0.01	5.3 ± 1.0
	S_p			ξ
$S_{pp}(Q)$	$(0.27 \pm 0.01) \times 10^{-20}$ cm^3			171 ± 1 Å

[a] Fixed parameters are shown without fitting errors.

correlation, which is defined as $\tilde{S}_{pp}(Q)$ in order to distinguish it from the total intensity of $S_{pp}(Q)$. The broken curve in Figure 7 exhibits the computed $\tilde{S}_{pp}(Q)$, which is almost the same magnitude as the experimentally obtained $S_{pp}(Q)$ and slightly less than $S_{pp}(Q)$ at low Q. The additional intensity for the reproduction of $S_{pp}(Q)$ was assumed to be caused by the polymer network, which can be described by a Lorentz function,[27] i.e.

$$S_{pp}(Q) = \tilde{S}_{pp}(Q) + S_0/(1 + \xi^2Q^2) \tag{24}$$

where S_0 is a prefactor and ξ is the correlation length (or blob size) of the polymer network. The solid curve in Figure 7 expresses the summation of $\tilde{S}_{pp}(Q)$ and $S_0/(1 + \xi^2Q^2)$, which can reproduce the experimental data very well. The dashed-dotted curve in Figure 7 shows $S_0/(1 + \xi^2Q^2)$ with $\xi = 171$ Å, and the dotted curve is the structure factor calculated by the equation in the square brackets in eq 18. In the case of the conventional hydrogels, the network size ξ is several tens of angstroms;[23] therefore, the 1 order of magnitude larger ξ of the NC gel is due to uniquely wide and homogeneous spatial distribution of the two-dimensional cross-linkers. It is mentioned that the obtained S_0 is 1 order of magnitude higher than that of our previous study near the sol−gel transition point.[13] Note that the contribution of polymer network was incoherently added in eq 24 by assuming that the coherence between the polymer network and the adsorbed polymer chains was negligible. The all fitting parameters are listed in Table 1.

5. Conclusion

The detailed structure of NC gels was revealed by contrast variation small-angle neutron scattering. The partial scattering function of clay, $S_{cc}(Q)$, confirmed that the clay nanoparticles exist without any aggregations. Then, the observed positive clay−polymer cross-term, $S_{cp}(Q)$, and the quantitative analysis proved that the polymer chains are strongly anchored at the surfaces of homogeneously dispersed clay nanoplatelets, and in this way the clay platelets can work as two-dimensional cross-

linkers. The density profile of adsorbed polymer segments perpendicular to the clay surface was evaluated by model fitting with $\phi(z) \propto 1 - (z/\zeta)^h$ (see eq 11), and $h \sim 5$ was obtained, which may reflect the strong attractive interaction between clay and polymer. The network size in NC gels, ξ, evaluated by eq 24 is uniquely wide compared to the conventional hydrogels with organic cross-linkers, which was confirmed by the analysis of the partial scattering function of polymer, $S_{pp}(Q)$. These characteristics are the origin of superior properties of NC gels.

The specific interactions between multicomponents can potentially create a variety of advanced properties as demonstrated by NC gels. Our sophisticated contrast variation method is quite efficient in order to investigate such multicomponent systems with nanoscale resolution, for the cross-terms can be uniquely observed.

Acknowledgment. This work was partially supported by the Ministry of Education, Science, Sports and Culture, Japan (Grants-in-Aid for Scientific Research (A), 2006−2008, No. 18205025, and for Scientific Research on Priority Areas, 2006−2010, No. 18068004). The SANS experiment was performed with the approval of Institute for Solid State Physics, The University of Tokyo, at Japan Atomic Energy Agency, Tokai, Japan.

References and Notes

(1) Utracki, L. A. *Clay-Containing Polymeric Nanocomposites*; Repra Tech. Ltd.: London, 2004.
(2) Okada, A.; Usuki, A. *Macromol. Mater. Eng.* **2006**, *291*, 1449–1476.
(3) Mann, S. *Biomineralization*; Oxford University Press: New York, 2001.
(4) Haraguchi, K.; Takehisa, T. *Adv. Mater.* **2002**, *14*, 1120–1124.
(5) Haraguchi, K.; Takehisa, T.; Fan, S. *Macromolecules* **2002**, *35*, 10162–10171.
(6) Haraguchi, K.; Farnworth, R.; Ohbayashi, A.; Takehisa, T. *Macromolecules* **2003**, *36*, 5732–5741.
(7) Haraguchi, K.; Li, H.-J.; Matsuda, K.; Takehisa, T.; Elliot, E. *Macromolecules* **2005**, *38*, 3482–3490.
(8) Shibayama, M.; Suda, J.; Karino, T.; Okabe, S.; Takehisa, T.; Haraguchi, K. *Macromolecules* **2004**, *37*, 9606–9612.
(9) Shibayama, M.; Karino, T.; Miyazaki, S.; Okabe, S.; Takehisa, T.; Haraguchi, K. *Macromolecules* **2005**, *38*, 10772–10781.
(10) Miyazaki, S.; Karino, T.; Endo, H.; Haraguchi, K.; Shibayama, M. *Macromolecules* **2006**, *39*, 8112–8120.
(11) Schmidt, G.; Nakatani, A. I.; Butler, P. D.; Han, C. C. *Macromolecules* **2002**, *35*, 4725–4732.
(12) Hecht, A.-M.; Horkay, F.; Geissler, E. *Phys. Rev. E* **2001**, *64*, 041402.
(13) Miyazaki, S.; Endo, H.; Karino, T.; Haraguchi, K.; Shibayama, M. *Macromolecules* **2007**, *40*, 4287–4295.
(14) Endo, H.; Schwahn, D.; Coelfen, H. *J. Chem. Phys.* **2004**, *120*, 9410–9423.
(15) Kotiarchyk, M.; Chen, S.-H. *J. Chem. Phys.* **1983**, *79*, 2461–2469.
(16) Milner, S.; Witten, T. A.; Cates, M. E. *Macromolecules* **1988**, *21*, 2619–2619.
(17) Percus, J. K.; Yevick, G. J. *Phys. Rev.* **1958**, *110*, 1–13.
(18) Thiele, E. *J. Chem. Phys.* **1963**, *39*, 474–479.
(19) Wertheim, M. S. *Phys. Rev. Lett.* **1963**, *10*, 321–323.
(20) Kinning, D. J.; Thomas, E. L. *Macromolecules* **1984**, *17*, 1712–1718.
(21) Shibayama, M.; Kawada, H.; Kume, T.; Matsunaga, T.; Iwai, H.; Sano, T.; Osaka, N.; Miyazaki, S.; Okabe, S.; Endo, H. *J. Chem. Phys.* **2007**, *127*, 144507–144513.
(22) Okabe, S.; Karino, T.; Nagao, M.; Watanabe, S.; Shibayama, M. *Nucl. Instrum. Methods Phys. Res., Sect. A* **2007**, *572*, 853–858.
(23) Shibayama, M.; Tanaka, T.; Han, C. C. *J. Chem. Phys.* **1992**, *97*, 6829–6841.
(24) Endo, H. *Physica B* **2006**, *385−386*, 682–684.
(25) Endo, H.; Allgaier, J.; Gompper, G.; Jakobs, B.; Monkenbusch, M.; Richter, D.; Sottmann, T.; Strey, R. *Phys. Rev. Lett.* **2000**, *85*, 102–105.
(26) Endo, H.; Mihailescu, M.; Monkenbusch, M.; Allgaier, J.; Gompper, G.; Richter, D.; Jakobs, B.; Sottmann, T.; Strey, R.; Grillo, I. *J. Chem. Phys.* **2001**, *115*, 580–600.
(27) Shibayama, M. *Macromol. Chem. Phys.* **1998**, *199*, 1–30.

MA800390P